Photoluminescence study of symmetry-related transitions in the spectrum of $Y_2O_3:Tb^{3+}$

Daniel den Engelsen, Jack Silver, Terry G. Ireland, George R. Fern, and Paul G. Harris

Centre for Phosphor and Display Materials, Wolfson Centre for Materials Processing, Brunel University London, Uxbridge, Middlesex, UB8 3PH, United Kingdom; jack.silver@brunel.ac.uk

Keywords: $Y_2O_3:Tb^{3+}$, Energy-transfer, Photoluminescence.

ABSTRACT

Herein we describe the results of a study on the photoluminescence of cubic nanosized $Y_2O_3:Tb^{3+}$. These results confirm our earlier conclusions based on cathodoluminescence about the energy flow from excited Tb^{3+} in a S_6 lattice site to Tb^{3+} in a C_2 site.

1. INTRODUCTION

The industrial applications of yttrium oxide doped with europium or terbium have stimulated scientists to investigate the energy flow in these materials upon excitation by electrons or UV-radiation. For cubic $Y_2O_3:Eu^{3+}$ a symmetry-related energy flow scheme was proposed in the 1980s [1, 2], while we have recently proposed such a scheme for $Y_2O_3:Tb^{3+}$ [3- 5]. The complicated nature of the spectrum of $Y_2O_3:Tb^{3+}$ impedes the assignment of the individual transitions in the $^4D_5 \rightarrow {}^7F_J$ (where J = 2, 3, 4, 5 and 6) clusters. Y_2O_3 doped with various concentrations of Tb^{3+} and annealed at temperatures above 950°C has the cubic structure of the mineral bixbyite. This cubic structure has two different Y^{3+} lattice sites, which possess the point symmetries C_2 and S_6: 24 lattice sites have C_2 symmetry, while the other 8 have S_6 symmetry [1-3]. From the concentration dependency of a few spectral lines of $Y_2O_3:Tb^{3+}$ we could assign these as being S_6; the majority of the spectral lines has C_2 symmetry [3]. The strongest S_6 line in the $Y_2O_3:Tb^{3+}$ spectrum is located in the $^4D_5 \rightarrow {}^7F_5$ cluster at 544.2 nm. This line and the strong C_2 line at 542.5 nm were the main targets for an in-depth study of the photoluminescence (PL).

Many authors have reported on the PL spectrum of $Y_2O_3:Tb^{3+}$; here we shall mention only the most relevant publications on the spectroscopic characteristics of $Y_2O_3:Tb^{3+}$. An important result in [3] was the doublet structure of the 542 nm and 544 nm lines, which became noticeable at a temperature of 103 K. A similar result was reported by Song and Wang [6], who also found 4 lines between 541 and 545 nm at 83 K. At 274 K these lines coalesced into two peaks, in which the 542 nm peak still showed a shoulder. Najafov et al. [7] showed the doublet structure of the 542 nm and 544 nm lines in the PL-spectra of $Y_2O_3:Tb^{3+}$ with various Tb^{3+} concentrations at room temperature, but they did not refer to these phenomena in their paper.

The excitation spectra of $Y_2O_3:Re^{3+}$ (Re^{3+} being a trivalent rare earth ion) were presented by Kano in the Phosphor Handbook [8]. The excitation band of $Y_2O_3:Tb^{3+}$ represented in Kano´s chapter shows two peaks, one at 304 nm and the other at 280 nm; however, it is not indicated which transitions were used to monitor these excitation spectra. Other reports on the excitation spectrum of $Y_2O_3:Tb^{3+}$ were given by Ropp [9], Najafov et al. [7], Muenchausen et al. [10], Meng et al. [11], Liu et al. [12], and Som et al. [13] Most authors assigned the broad excitation band between 260 nm and 310 nm to a $4f^8 \rightarrow 4f^7 5d^1$ transition in the Tb^{3+} ion. We shall adopt here the assignment of Kano [8]: the excitation band between 260 nm and 340 nm is due to $4f^8 \rightarrow 4f^7 5d^1$ transitions, since the CT band of $Y_2O_3:Tb^{3+}$ is positioned at 64000 cm^{-1} (156 nm) in the VUV. These assignments were confirmed by Dorenbos, see for instance [14]. No attention was paid in the papers [6, 7, 9-13] to symmetry-related transitions and effects in the spectrum of $Y_2O_3:Tb^{3+}$, mainly because the lines at 542 nm and 544 nm in the emission PL spectra were not observed as split (due to poor resolution of the spectrometers) or their behaviour was overlooked and thus, not taken into consideration. Laser-excited spectra of photonic band gap $Y_2O_3:Tb^{3+}$ materials were reported by Withnall et al. [15] in a temperature range from 25-400°C. These temperatures were too high to split the $Y_2O_3:Tb^{3+}$ $^5D_4 \rightarrow {}^7F_5$ doublets at 542 nm and 544 nm.

2. MATERIALS AND EQUIPMENT

The nanometre sized $Y_2O_3:Tb^{3+}$ phosphor particles were synthesized by the urea method, described in our earlier work [3]. The Tb^{3+} concentration was varied between 0.1 and 10% (mol ratio versus Y^{3+}. Figure 1a shows a scanning transmission electron microscope (STEM) image of 0.1% $Y_2O_3:Tb^{3+}$ at -171.3° C and beam energy of 200 keV. The particle size varied from 130 to 200 nm in this sample; the samples with larger Tb^{3+} concentration had smaller particle size.

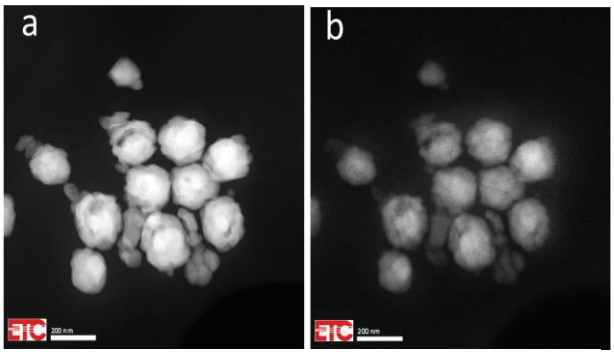

Figure 1. a: STEM image of 0.1%$Y_2O_3:Tb^{3+}$ at 200 keV and -171°C. b: Panchromatic CL image of same area.

The almost spherical particles consist of smaller crystallites, which have dimensions of about 40 nm. Figure 1b is the panchromatic cathode luminescence (CL) image of the same area as represented in Figure 1a. Figures 1a and 1b were

recorded with a STEM, model 2100F, JEOL, Japan, equipped with a Vulcan™ CL detector, Gatan, USA, for imaging and spectroscopic purposes. Details of this equipment have been described previously [3]. The PL spectra were collected at room temperature using a Bentham M300 programmable grating monochromator photometer system with computer controlled wavelength scanning and intensity data collection, using in the visible region an 1800 lines/mm grating and 0.37 mm slits.

3. RESULTS

Figure 2 shows two PL spectra of 1% Y_2O_3:Tb^{3+} between 460 and 700 nm: one excited at 282 nm and the other excited at 305 nm. The $^5D_4 \rightarrow {}^7F_J$ (J=1, 2…6) transition clusters are indicated in this figure. The spectra excited at 282 nm and 305 nm are different, although not so noticeable in Figure 2. In Figure 3 the

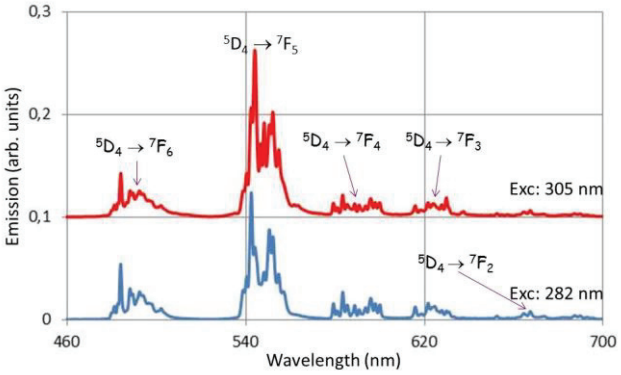

Figure 2. PL spectra of 1% Y_2O_3:Tb^{3+} excited at 282 and 305 nm.

relevant differences are clearly shown for the $^5D_4 \rightarrow {}^7F_5$ transition cluster. Exciting cubic Y_2O_3:Tb^{3+} with radiation between 260 nm and 285 nm wavelength results in mainly C_2 type emission lines, whereas excitation at 305 nm enhances the S_6 type emission lines. This symmetry-related assignment is based on the analyses of the CL spectra reported earlier [3]: the peak at 542.8 nm was identified as C_2 and the peak at 544.4 nm as S_6.

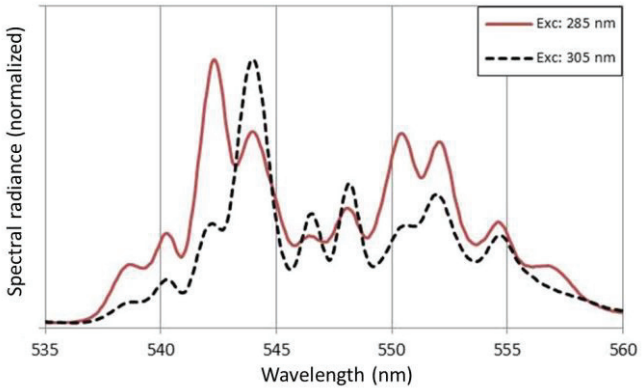

Figure 3. Overlay of PL spectra of $^5D_4 \rightarrow {}^7F_5$ transition cluster of 0.3% Y_2O_3:Tb^{3+} excited at 285 nm and 305 nm.

The spectra in Figure 3 have been normalised to the highest peak in each spectrum to enhance the differences. Exciting 0.3% Y_2O_3:Tb^{3+} between 260 nm and 285 nm enhances the peak at 542.8 nm rather than the peak at 544.4 nm, whereas excitation at 305 nm reverses the outcome. From a study of the CL-spectra of Y_2O_3:Tb^{3+} recorded with a transmission electron microscope it is known that the peaks at 542.8 and 544.4 nm are doublets [3]. By using 0.1mm slits in the Bentham monochromator the signal reduced too much to observe the splitting of the 542.8 and 544.4 nm lines at room temperature.

Excitation spectra of Y_2O_3:Tb^{3+} between 250 nm and 350 nm monitored at 542.8 and 544.4 nm are represented in Figures 4a and 4b respectively. The spectra shown in Figures 4a and 4b are quite different at low Tb^{3+} concentrations, whilst at high Tb^{3+} concentration they show a tendency to become more equal. In Figure 4a the maximum is at about 282 nm, while Figure 4b shows a maximum at 305 nm. The excitation spectrum of 10% Y_2O_3:Tb^{3+} manifests a small absorption band at 338 nm, which is not noticeable in the spectra of the other Y_2O_3:Tb^{3+} samples. The excitation spectra represented in Figures 4a and 4b can be deconvoluted with two Gaussian profiles, E1 and E2, as shown for 0.1%Y_2O_3:Tb^{3+}in Figures 4c and 4d respectively. The algorithm for a Gaussian-type deconvolution has been described previously [3]. The Gaussian profiles were fitted to the experimental spectra with a least squares algorithm. The E1-peak is broader than the E2 peak. Najafov et al.[7] and Som et al. [13] also made a Gaussian deconvolution of the excitation band for Y_2O_3:Tb^{3+} between 250 nm and 340 nm. They also found that the E2 peak was

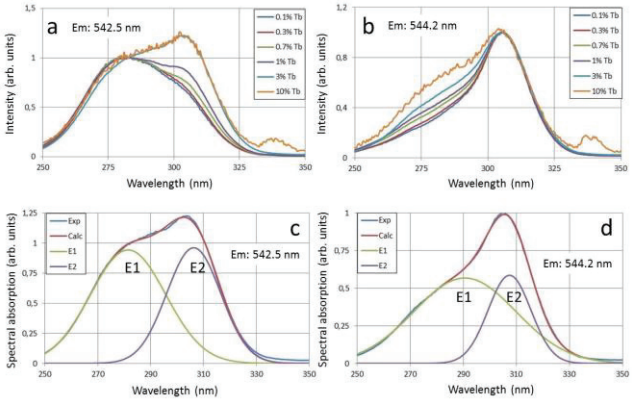

Figure 4. Excitation spectra of Y_2O_3:Tb^{3+} a: monitored at 542.8 nm. b: monitored at 544.4 nm. c: Deconvolution of 0.1% Y_2O_3:Tb^{3+} C_2-type spectrum; d: Deconvolution of 0.1% Y_2O_3:Tb^{3+} S_6-type spectrum.

narrower than the E1-peak. Som et al. [13] estimated the full width at half maximum (FWHM) of E1 and E2 at 0.45 eV and 0.26 eV respectively. These values are smaller than our results, which are 0.58 eV and 0.29 eV. In Figure 5 we have plotted the ratio between the integrated absorptions (IA) of E1 and E2, viz. IA_{E1}/IA_{E2}, as a function of the Tb^{3+} concentration. Integrated absorption refers to the area under the E1 or E2 peaks. We assign the E1 peak in Figures 4c and 4d to the $^7F_6 \rightarrow {}^9D_J$ (C_2) excitation and the E2 peak to the $^7F_6 \rightarrow {}^9D_J$ (S_6) excitation, in which the ^9D_J levels have the $4f^7 5d^1$ electron configuration.

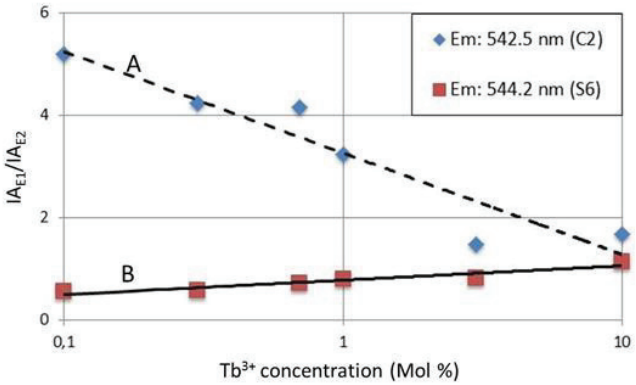

Figure 5. Ratio of integrated absorption (IA) of peaks E1 and E2 in the excitation spectra of Y_2O_3:Tb^{3+}. Line A refers to the excitation spectra monitored at 542.8 nm, while line B refers to the excitation spectra monitored at 544.4 nm.

In the case of monitoring the emission at the S_6-transtion at 544.4 nm (line B), we see a slight increase of the E1-peak (C_2-type) with Tb^{3+} concentration in Figure 4d and Figure 5. Figure 4a shows an increase of S_6-characteristics with Tb^{3+} concentration, which is also clearly reflected in Figure 5 by the negative slope of line A, indicating the decreasing IA_{E1}/IA_{E2} ratio monitored at 542.8 nm.

PL spectra of the $^5D_4 \rightarrow {}^7F_5$ transition cluster are depicted in Figure 6: Figure 6a shows the spectra excited at 282 nm, while Figure 6b shows the spectra excited at 305 nm. For comparison reasons these spectra have been normalised: at 542.8 nm for Figure 6a and at 544.4 nm for Figure 6b.

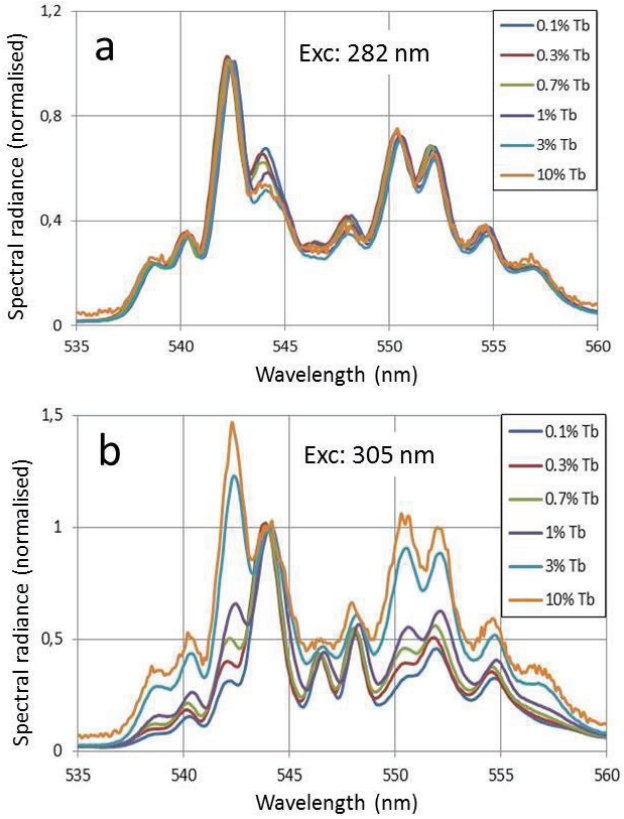

Figure 6. PL spectra of the $^5D_4 \rightarrow {}^7F_5$ transition cluster of Y_2O_3:Tb^{3+} at various Tb^{3+} concentrations. a: Excited at 282 nm and normalised at 542.8 nm. b: Excited at 305 nm and normalised at 544.4 nm.

The differences between the spectra in Figures 6a and 6b are large: Figure 6a shows only a modest concentration effect, whereas the concentration effect in Figure 6b is substantial. The peak at 544.4 nm is not the only one that shows S_6 character, the peaks at 548.1 nm, 550.3 nm and 552 nm also show S_6 characteristics, albeit less than the peak at 544.4 nm. This can be concluded from the variations shown in Figure 6b. The symmetry-related effects as shown in Figure 6 are most pronounced for the $^5D_4 \rightarrow {}^7F_5$ transition cluster, for the other transition clusters these are less. The analysis of the concentration effect shown in Figure 6b requires a deconvolution of the measured spectra. This deconvolution was done with Lorentzian profiles. The reason for choosing Lorentzian profiles is that the peaks at 542.8 nm and 544.4 nm peaks are doublets. The latter are better represented with Lorentzian profiles, which are narrow at spectral radiances > half maximum and broad at the bottom. An example of the deconvolution of the $^5D_4 \rightarrow {}^7F_5$ peaks at 542.8 nm and 544.8 nm is shown in Figure 7 for 1% Y_2O_3:Tb^{3+}. In this deconvolution seven Lorentzian profiles were used. The amplitudes of these seven profiles were fitted to the measured PL spectrum with a least squares algorithm using Microsoft´s Excel Solver software. The seven Lorentzian profiles that represent the measured spectrum are indicated in Figure 7 as p1, p2,…p7. The most relevant are p2, p3, p5 and p6, because the radiances of these peaks are used for further analyses.

The radiance ratio $I_{542.8}/I_{544.2}$ has been plotted in Figure 8 as a function of the Tb^{3+} concentration, where $I_{542.5}$ is the sum of radiances of p2 and p3 and $I_{544.2}$ is the sum of the radiances of p5 and p6. The correspondence between Figure 8, derived from the PL spectra, and the equivalent Figure 9 in [3], based on CL spectra, is excellent.

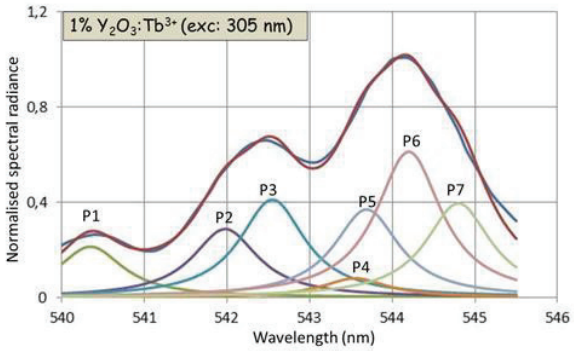

Figure 7. Deconvolution of a part of the $^5D_4 \rightarrow {}^7F_5$ spectrum between 540 and 546 nm with seven Lorentzian profiles (p1, p2, …p7).

The knee of the PL curve in Figure 8 is at about 0.7%Tb^{3+}; this coincides with the knee in Figure 9a of [3]. In that publication we described a relation between the average distance D_{Tb} between two Tb^{3+} ions in the Y_2O_3 lattice and the Tb^{3+} concentration has been given. At 0.7 Mol % Tb^{3+} D_{Tb} is 1.7 nm, hence from the PL-measurements we also find that the critical distance, $D_{Tb^{3+}}^{Crit}$, for interaction between the S_6 and C_2 sites is 1.7nm. It should be stressed that the curve in Figure 8 is based on the Figure 6b: excitation at 305 nm, which means excitation of Tb^{3+} at S_6 lattice sites.

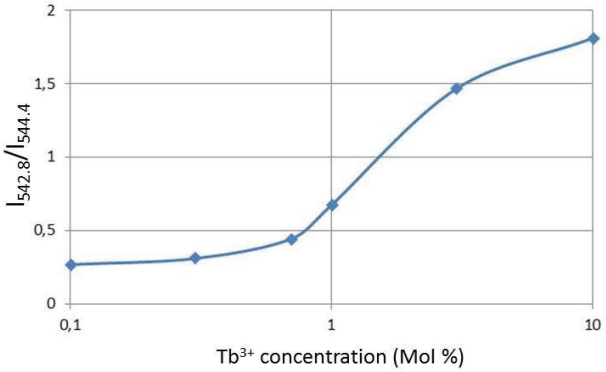

Figure 8. Radiance ratio of peaks at 542.8 and 544.4 versus Tb^{3+} concentration (excited at 305 nm).

Figure 9 shows the energy levels based on the assignments for the excitation bands between 250 nm and 340 nm and the strongest emission peaks in the $^5D_4 \rightarrow {}^7F_5$ transition cluster of Y_2O_3:Tb^{3+}. Figure 9a is an overall picture, whereas Figure 9b zooms in on the main peaks of the $^5D_4 \rightarrow {}^7F_5$ transition cluster. Based on the analyses of the CL spectra of Y_2O_3:Eu^{3+}

[16], we have assigned the 542.8 nm and 544.4 nm peaks (indicated at 542.45 nm and 544.17 nm respectively in Figure 9b) in the spectrum of Y_2O_3:Tb^{3+} as C_2 and S_6 respectively [3]. It is tempting to make the same assignment for the excitation spectrum, viz. the peaks E1 and E2 in Figures 4c and 4d. In doing so, E1 represents a C_2 excitation peak and E2 a S_6 peak, as mentioned before.

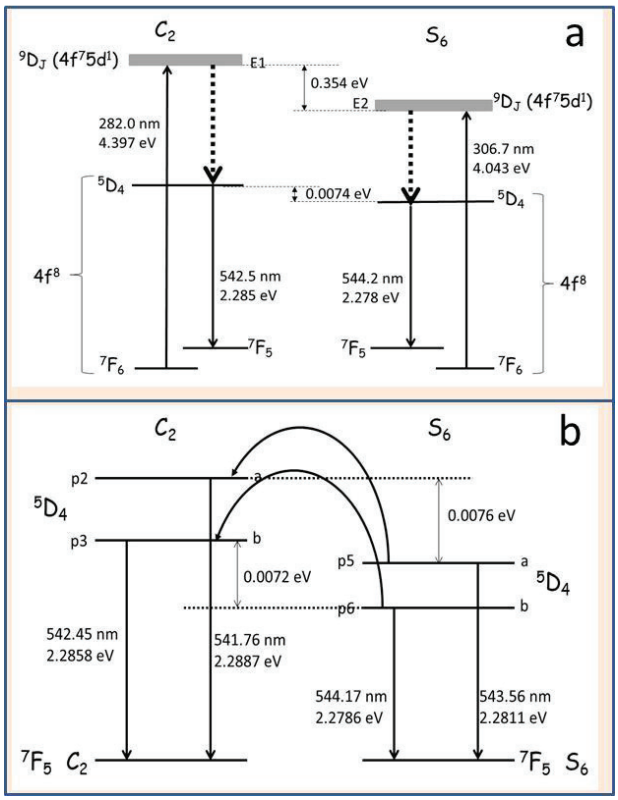

Figure 9. Energy levels involved in the excitation band and $^5D_4 \rightarrow {}^7F_5$ transition cluster of Y_2O_3:Tb^{3+}. a: Excitation mechanism; E1 and E2 refer to the peaks shown in Figure 5. b: Energy transfer from $^5D_4$ (S_6) to $^5D_4$ (C_2). For reasons of clarity the energy scale has been distorted.

4. CONCLUSIONS

The identification of symmetry-related transitions in the PL-spectrum of Y_2O_3:Tb^{3+} allowed the determination of the energy flow from excited Tb^{3+} in a S_6 lattice site to Tb^{3+} in a C_2 site. The results obtained from the PL-spectra agree favourably with the results from our earlier CL-work. For such a well-known and well-studied phosphor as Y_2O_3:Tb^{3+} it was surprising that we could not find any symmetry-related analysis of the CL and PL spectra of Y_2O_3:Tb^{3+} in the literature.

5. REFERENCES

[1] M. Buijs, A. Meyerink, and G. Blasse, "Energy Transfer between Eu^{3+} Ions in a Lattice with two Different Crystallographic Sites: Y_2O_3:Eu^{3+}, Gd_2O_3:Eu^{3+} and Eu_2O_3", J. Lumin., 37, 9-20 (1987).

[2] D.B.M. Klaassen, R.A.M. van Ham, and T.G.M. van Rijn, "Energy Transfer Processes in Yttrium Oxide Activated with Europium", 43, 261-274 (1989).

[3] D. den Engelsen, P. G. Harris, T. G. Ireland, G. Fern, and J. Silver, "Symmetry-Related Transitions in the Spectrum of Nanosized Cubic Y_2O_3:Tb^{3+} ", ECS J. Solid State Sci. Technol., 4, R105-R113, 2015.

[4] D. den Engelsen, P. G. Harris, T. G. Ireland, G. Fern, and J. Silver, "Symmetry-Related Transitions in the Spectrum of Nanosized Cubic Y_2O_3:Tb^{3+}: Part 2", ECS J. Solid State Sci. Technol., submitted.

[5] D. den Engelsen, G.R. Fern, T.G. Ireland, P.G. Harris, and J. Silver, "Transmission electron microscope study of symmetry-related transitions in cubic Y_2O_3:Tb^{3+}", Eurodisplay, Ghent, September 21-23 (2015).

[6] H. Song and J. Wang, "Dependence of photoluminescent properties of cubic Y2O3:Tb^{3+} nanocrystals on particle size and temperature", J. Lumin., 118, 220-226 (2006).

[7] H. Najafov, Y. Satoh, S. Ohshio, A. Kato and H. Saitoh, "Luminescence properties of Y_2O_3:Tb^{3+} whiskers fabricated by chemical vapor deposition", Jpn. J. Appl. Phys., 43, 7111-7119 (2004).

[8] T. Kano in Phosphor Handbook, 2nd ed., W. Yen, S. Shionoya and H. Yamamoto eds., p. 197-198, CRC Press, Boca Raton (2007).

[9] R.C. Ropp, "Spectral properties of rare earth oxide phosphors", J. Electrochem. Soc., 111, 311-317 (1964).

[10] R.E. Muenchausen, L.G. Jacobsohn, B.L. Bennett, E.A. McKigney, J.F. Smith, J.A. Valdez and D.W. Cooke, "Effects of Tb doping on the photoluminescence of Y_2O_3:Tb nanophosphors", J. Lumin., 126, 838-842 (2007).

[11] Q. Meng, B. Chen, W. Xu, Y. Yang, X. Zhao, W. Di, S. Lu, X. Wang, J. Sun, L. Cheng, T. Yu and Y. Peng, "Size-dependent excitation spectra and energy transfer in Tb^{3+} - doped Y_2O_3 nanocrystalline", J. Appl. Phys., 102, 093505-1- 093505-6 (2007).

[12] Z. Liu, L. Yu, Q. Wang, Y. Tao and H. Yang, "Effect of Eu,Tb codoping on the luminescent properties of Y_2O_3 nanorods", J. Lumin., 131, 12-16 (2011).

[13] S. Som, S. Dutta, Vijay Kumar, Vinod Kumar, H.C. Swart and S.K. Sharma, "Swift heavy ion irradiation induced modification in structural, optical and luminescence properties of Y_2O_3:Tb^{3+} nanophosphor", J. Lumin., 146, 162-173 (2014).

[14] A. Dobrowolska, E.C. Karsu, A.J.J. Bos and P. Dorenbos, "Spectroscopy, thermoluminescence and afterglow studies of $CaLa_4(SiO_4)_3O$:Ln (Ln = Ce, Nd, Eu, Tb, Dy)", J. Lumin., 160, 321-327 (2015).

[15] R. Withnall, M.I. Martinez-Rubio, G.R. Fern, T.G. Ireland and J. Silver, "Photonic phosphors based on cubic Y_2O_3:Tb^{3+} infilled into a synthetic opal lattice" J. Opt. A: Pure Appl. Opt., 5, S81-S85 (2003).

[16] D. den Engelsen, P. G. Harris, T. G. Ireland and J. Silver, "Cathodoluminescence of nanocrystalline Y_2O_3:Eu^{3+} with various Eu^{3+} concentrations", ECS J. Solid State Sci. Technol., 4, R1-R9 (2015).